Load transfers and arching effects in granular soil layer

Bastien Chevalier, Gaël Combe & Pascal Villard

Laboratoire 3S-R : Sols, Solides Structures et Risques
BP 53 - 38041 Grenoble cedex 9 France
bastien.chevalier@ujf-grenoble.fr

Abtract :
Load transfer and other arching effects are mechanisms frequently met in civil engineering structures, and particularly in geotechnical earth structures such as piled embankments or karstic subsidence… The proposed study focuses on the numerical discrete analysis of granular material response submitted to specific boundary conditions leading to load transfer (embankment built over a trench or over a network of piles). The influence of several parameters has been studied: granular layer thickness, friction behaviour and particle shapes. Various load transfer mechanisms are observed depending on the boundaries and also on the granular layer properties. The comparison between three dimensional Discrete Element Modelling and analytical calculation methods leads to a various agreement depending on the case treated.

Résumé :
Les transferts de charge et autres effets voûtes sont des mécanismes souvent rencontrés dans les ouvrages de génie civil et notamment en géotechnique : renforcement de sols par inclusions, effondrement karstique…Cette étude repose sur l'analyse numérique discrète de la réponse d'un matériau granulaire à des sollicitations conduisant à des transferts de charge (cas d'un remblai sur une tranchée et sur inclusions). L'influence de l'épaisseur de matelas granulaire, du comportement en frottement et de la forme des particules constituant le matériau granulaire ont été étudiés. La variation de ces paramètres conduit à l'observation de mécanismes très différents. Une comparaison des résultats des simulations numériques avec quelques méthodes de dimensionnement a été effectuée et se traduit par des niveaux de concordance divers selon la configuration traitée.

Key-words :
load transfer, granular layers, DEM

1 Introduction

Load transfer and other arching effects are mechanisms frequently met in civil engineering, and particularly in geotechnical earth structures such as piled embankments, embankments submitted to karstic subsidence… A great variety of analytical or empirical approaches have been developed: some consider particular shear planes for load transfer (Terzaghi (1943)) others take into account the formation of idealized arches of different shapes (Hewlett and al (1988), Low and al (1994), EBGEO (1997)). Besides the structures geometry, one parameter, commonly used and having a great influence on the load transfer, is the internal friction angle of the soil embankment. The predicted results of the analytical methods used vary greatly from one to another.

This study focuses on the numerical response of a particles assembly submitted to specific boundary conditions leading to load transfer over a trench or over a network o piles. The 3D Distinct Element Method used, allows reproducing the behaviours of granular materials (particles reorganization, collapse, dilatancy…). The purpose of this study is to highlight the arching effects and to obtain an analytical formulation taking into account more realistic mechanisms.

2 Numerical model and procedures

2.1 Distinct Element Method

The Distinct Element Method used in this study is based on the well known molecular dynamics approach. The granular material is modelled with grains interacting with each other. Normal linear contact law defined by a stiffness parameter k_n is considered. An incremental tangential contact law based on the elastic perfectly plastic model proposed by Cundall and al (1979). This law is defined by a tangential stiffness k_s and a Coulomb friction criterion (coefficient μ). The discrete element program used is a three dimensional software (SDEC, Donzé and Al (1997)).

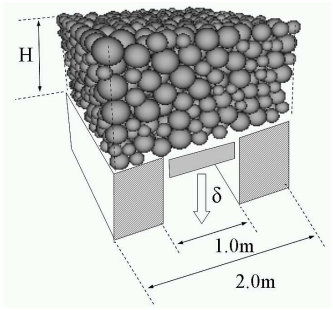

Fig. 1: Soil layer over a trench

2.2 Geometry of the numerical model

A granular layer is laid in a box delimited by frictionless rigid walls. The load transfer mechanisms are obtained under gravity by moving a delimited part of the horizontal bottom wall. This plate is moved by increments δ_i. The total displacement is $\delta=\Sigma\delta_i$. The fixed parts of the bottom wall called supports have a friction coefficient μ.

Two different applications have been studied. The first pattern (Fig. 1) reproduces the example of a granular layer built over a trench. The second pattern (Fig. 2) deal with the numerical modelling of an embankment built on a soft soil reinforced by inclusions.

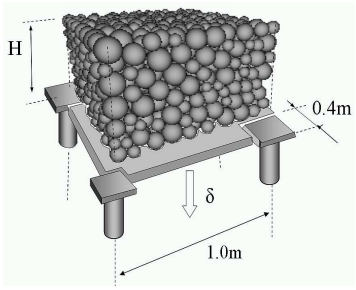

Fig. 2: Soil layer over piles

2.3 Physical properties of the granular layer

Two grading have been studied. The first called G1 is only composed of spheres. The second one called G2 is composed of two jointed particles of same diameter called cluster. The distance between the two jointed spheres centers is 95% of their diameter. The particle sizes are uniformly distributed between minimal and maximal diameters d_{min} and $d_{max}=4d_{min}$. The number of particles is constant and equal to 8000 per m^3.

Three dense and cohesionless granular layers (porosity $\eta=0.355$) called *mi* (*i=1…3)* are obtained from the grading G1 and G2, according to various micromechanical parameters sets (Tab. 1). Each *mi* have the same rigidity level $\kappa=<k_n>/(<d>P)=800$, Combe and al (2003), where $<k_n>$ is the average normal contact stiffness, $<d>$ the average diameter of the particles and P the isotropic pressure level. The mechanical characteristics have been determined by leading a numerical modelling of a triaxial test under an initial low isotropic pressure of 16 kPa.

	m1	*m2*	*m3*
grading	G1	G2	G2
porosity	0.355		
grain density ($kg.m^{-3}$)	2650		
apparent density ($kg.m^{-3}$)	1600		
κ	800		
k_s/k_n	0.75		
μ	0.577	0.176	0.364
Young modulus (MPa)	9.2	12.9	11.2
Poisson coefficient	0.12	0.11	0.11
peak friction angle φ_{peak}	27°	27°	39°
residual friction angle	22.3°	24.7°	29.5
dilatancy angle ψ	28°	24°	41°

Tab. 1: Characteristics of the numerical granular assembly

3 Application to embankment over a trench

This part of the study deals with the theoretical case treated by Terzaghi (1943), illustrated on Fig. 1, which defines the stress q applied on the mobile plate by:

$$q = \frac{L \quad \gamma}{2 \quad K_a \tan\varphi} \quad \left(1 - e^{-\ K_a \tan\varphi \quad 2 \quad H/L}\right) \qquad (1)$$

where L is the width of the trench, K_a=(1-sin φ)/(1+sin φ) the active earth pressure coefficient, H the granular layer thickness, φ the friction angle and γ the apparent density of the granular layer.

3.1 Influence of the shape of the particles

The modelled granular materials *m1* and *m2* are respectively composed of spherical particles and clusters. The efficacy of a granular layer built over a subsiding trench is define by Terzaghi (1943): $E_T=1-W_B/W$ where W_B is the resulting vertical force applied on the mobile plate and W is the weight of the granular layer situated just over the trench. The maximal efficacy of the granular layer is given on Fig. 3 for different values of H. The efficacies calculated from Ter43 are also represented. The efficacy reaches a maxima and then decreases when δ increases.

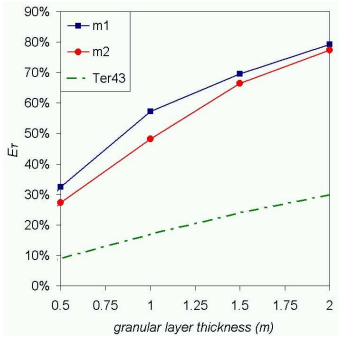

Fig.3: Efficacy of the granular layer m1, m2 over a trench

The efficacies obtained with *m2* are lower than those obtained with *m1*. However, when granular thickness exceeds 1 m, this difference between the two models is smaller. Until the appearance of an arch, the sliding planes intersect below the supports with *m2* as they intersect above the supports with *m1* (Fig. 4). After an arch is formed, the efficacies naturally converge but the sliding pattern is still different and perhaps related to the dilatancy angles ($\psi(m1)$=28°; $\psi(m2)$=24°).

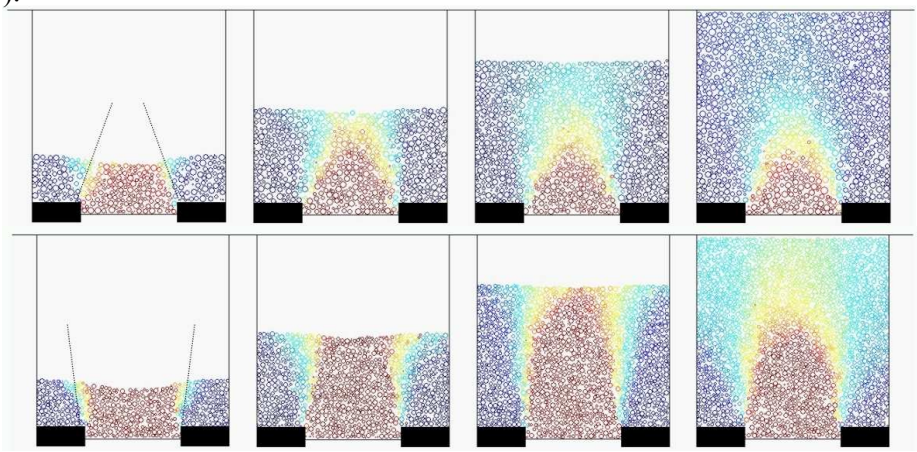
Fig.4: *m1* (up) and *m2* (down) particles displacements in a cross-section of the granular layer (δ=0.12m). (dark blue=no displacement / dark red = 0.12m displacement)

In order to analyse the numerical results, two particles families can be defined (Fig. 5): particles located along (Δ) vertical axis above support and particles located along (Δ') vertical axis above mobile plate. For these two particles families, the Z-axis positions versus the total displacement have been represented on Fig. 6 for δ=0.12 m. A critical height exists above which the variations of the vertical displacements of the particles are rather the same (with a 3cm threshold) for the two particle families. The particles assembly over the so called *limit of equal settlement* moves as a unique solid.

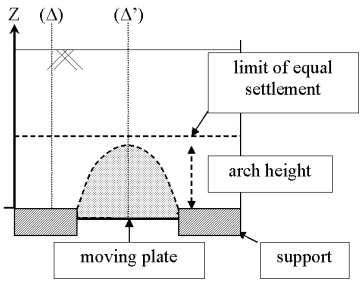

Fig.5: Definition of the *limit of equal settlement*

When H→∞ in eq. (1), an analytical maximal stress q_{max} can be calculated and converted into an equivalent arch height $h_{eq}=L/(2K_a\tan\varphi)$. ($h_{eq}=1.5$ *m* in the present case). The results of numerical and analytical models diverge with regard to the efficacies (Fig. 3) but also with

		m1	*m2*
limit of equal settlement	numerical results	1.13m	1.02m
	Analytical results	1.5m	1.5 m
surface settlement for H=2.0m		0.02 m	0.03 m

Tab. 2: Numerical and analytical settlement with *m1* and *m2*. *Moving plate displacement: δ=0.12m.*

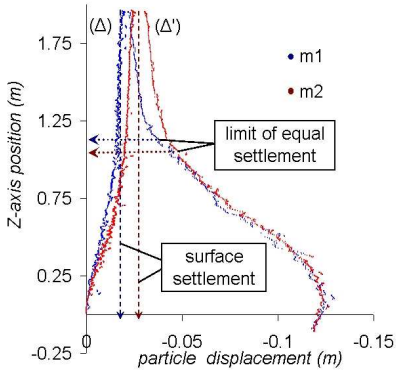

Fig. 6: Vertical displacements along (Δ) and (Δ') axis (δ=0.12m)

regard to the mechanisms descriptions (Tab.2). It seems that the initial numerical granular porosity may influence the arching effect. Looser granular layer should be tested in order to appreciate the effect of weaker dilatancy on the difference between numerical results and the analytical model of Terzaghi, eq. (1).

The influence of the shape of the particles is not really significant in this case with regard to the efficacy of the granular layer, Fig. 3. However, even if the mechanism of arching seems to be similar in both cases for great value of layer thickness, the global subsiding of the granular material is much more important (Fig.4 and 6) with *m2* (0.03 m) than with *m1* (0.02 m).

3.2 Influence of the peak friction angle

The compared modelled materials are *m2* and *m3, Tab. 1*. The only varying parameter is φ_{peak} only depending on μ in this case: $\varphi_{peak}(m2)$=27° and $\varphi_{peak}(m3)$=39°. With *m3*, the efficacy increases with δ and then stabilizes.

We can notice on Fig.7 the divergence between the numerical results and predicted efficacies obtained from the theory of Terzaghi. Numerical modelling leads again to greater efficacies. When φ_{peak} increases, the efficacy of the granular layer increases (Fig.7).

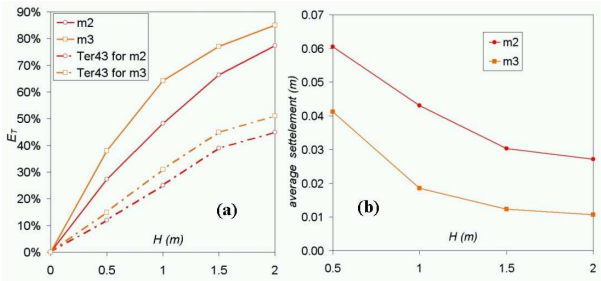

Fig. 7: Efficacy (a) and surface settlement (b) of the granular layer *m2*, *m3* over a trench

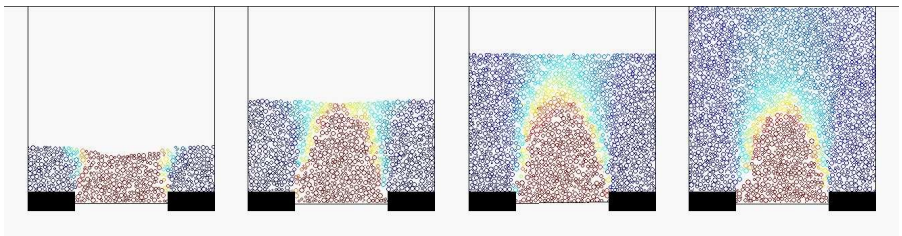

Fig. 8: *m3* particle displacements in a cross-section of the granular layer (δ=0.12 m). (dark blue=no displacement / dark red = 0.12 m displacement)

The limit of equal settlements is not influenced by the value of φ_{peak},. A greater φ_{peak} induces lower surface settlements (Fig.7).

4 Application to embankment over a network of piles

The pattern modelled in this study represents a 1.0m square mesh of structure. Each support (0.2mx0.2m) situated at the corner of the mesh (Fig. 2) represents a quarter of a pile cap. The materials *m1*, *m2*, *m3* have been tested in this application, the granular layer thickness varying between 0.5m and 2.0m. The behaviour of each material is assessed by an efficacy

defined by: $E_P=W_P/W_T$, where W_P is the vertical force applied on the piles and W the total weight of the granular material involved. The values obtained by numerical modelling will be compared to these given by two existing analytical methods taking into account the formation of hemispheric arches over a network of piles, Hewlett and Al (1988) and EBGEO (1997).

4.1 Influence of the shape of the particles

The difference between efficacies obtained with *m1* and *m2* granular layer is less than 5% (Fig.9). Numerical results give higher efficacies of the granular layer than the two analytical methods. The displacements field in a vertical plane (Fig. 8) for different thicknesses show that the kinematics of the granular layer is very different over a network of piled than over a trench. No real arch is formed (Fig11). The limit of equal settlement (Fig. 10) occurs for 0.37m Z-axis position. A part of the granular layer located above this limit lay on immobile pyramidal shaped portion of granular material, located on each support. This block of soil would completely flow below if the mobile plate had been removed. The surface settlements (Fig. 10) are 0.08m for *m1* and 0.085m for *m2*, for δ=0.12m.

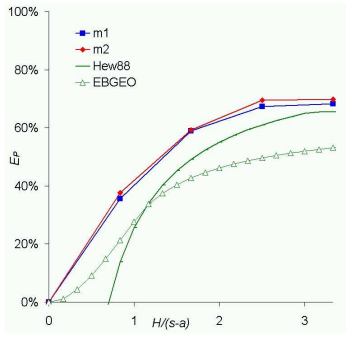

Fig.9: Efficacy of the granular layer *m1*, *m2* over a network of piles (φ=27°); (*s*-*a*=0.60m)

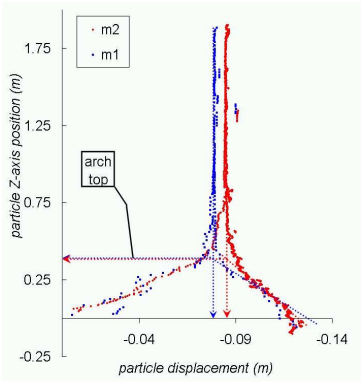

Fig.10: Displacement profiles along (Δ) and (Δ') axis (δ=0.12m)

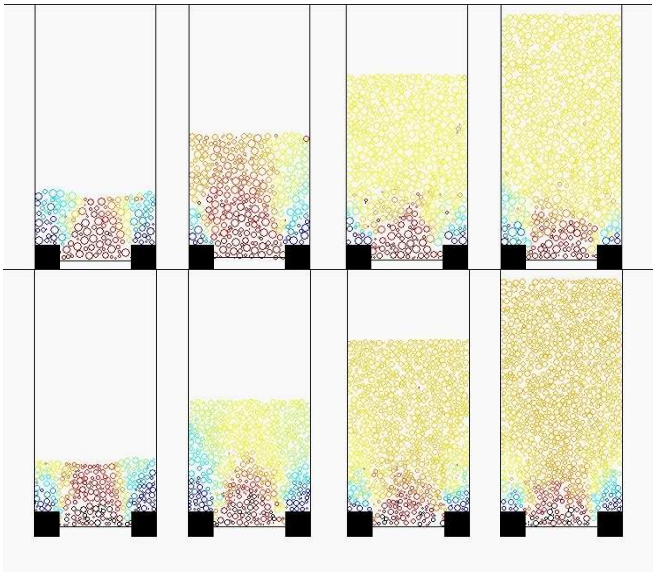

Fig.11: *m1* (up) and *m2* (down) particles displacements in a cross-section of the granular layer (δ=0.12m). (dark blue=no displacement / dark red = 0.12m displacement)

4.2 Influence of friction angle

The load transfer increases greatly with φ_{peak} (Fig.13). For H=2.0m, 69% of the *m1* and *m2* granular material weight are transferred to the piles while 89% are transferred with *m3*. With regard to the kinematics (Fig.12), the mechanism involved with *m3* is the same as previously, only the displacement of the block located over the equal settlement limit decreases (0.06m for H=2.0m).

The position of the equal settlement limit (0.38m above pile top) is not influenced by particles shape or friction coefficient, in these cases.

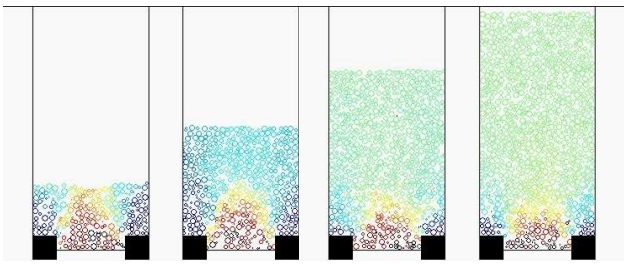

Fig.12: *m3* particles displacements in a cross-section of the granular layer (δ=0.12m). (dark blue=no displacement / dark red = 0.12m displacement)

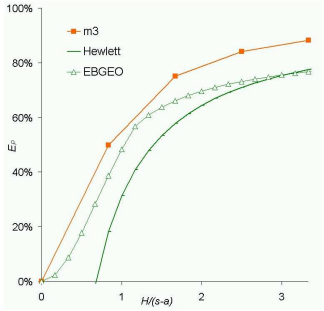

Fig.13: Efficacy of the granular layer *m2*, *m3* over a network of piles; *(s-a)*=0.60m

5 Conclusion

The friction behaviour is clearly one of the essential parameters influencing the load transfer efficacies. However, the way how this friction behaviour is taken into account in the theoretical methods can lead to very different results. The divergence between theoretical and the numerical results is significant for the trenches while a good agreement exist in the case of granular layer built over a network of piles. The load transfer kinematics – and the appearance of arches - are also very dependent on friction behaviour and on boundary conditions (case of trench or network of piles). The influence of the dilatancy angle had to be clarified. An experimental apparatus involving various real granular materials (sand, gravel …) over a trench is in preparation. The expected experimental results will help us in the calibration of our numerical model for further comparison with other analytical approaches.

References

- Terzaghi, K. 1943. *Theoretical soil Mechanics*. New York, Wiley.
- Hewlett, W.J. and Randolph, M.F. 1988. Analysis of piled embankment, *Ground engineering*, **21**(3): 12-18.
- Low, B.K., Tang, S.K. and Choa, V. 1994. Arching in piled embankments, *Journal of Geotechnical and Geoenvironmental Engineering*, **120**(11): 1917-1938.
- Donzé, F.V. & Magnier, S.-A. 1997. Spherical Discrete Element Code. In: *Discrete Element Project Report no. 2*. GEOTOP, Université du Québec à Montréal.
- Combe G. and Roux J.-N. 2003. Discrete numerical simulation, quasi-static deformation and the origin of strain in granular materials. 3ème Symp. Int. sur le Comportement des sols et des roches tendres, Lyon, 22-24 Septembre 2003, In Di Benedetto et al., pp 1071-1078.
- Cundall P.A. and Strack O.D.L. 1979. A discrete numerical model for granular assemblies. *Géotechnique*, **29**(1):47-65
- EBGEO, 1997: Empfehlungen für Bewehrungen aus Geokunststoffen. *Deutsche Gesellschaft fürGeotechnik* (Hrsg.) Verlag Ernst&Sohn, Berlin, Germany.